

# Effects of wildland fire smoke on a tree-roosting bat: integrating a plume model, field measurements, and mammalian dose–response relationships

M.B. Dickinson, J.C. Norris, A.S. Bova, R.L. Kremens, V. Young, and M.J. Lacki

**Abstract:** Faunal injury and mortality in wildland fires is a concern for wildlife and fire management although little work has been done on the mechanisms by which exposures cause their effects. In this paper, we use an integral plume model, field measurements, and models of carbon monoxide and heat effects to explore risk to tree-roosting bats during prescribed fires in mixed-oak forests of southeastern Ohio and eastern Kentucky. Tree-roosting bats are of interest primarily because of the need to mitigate risks for the endangered Indiana bat (*Myotis sodalis*), our focal species. Blood carboxyhemoglobin concentrations predicted from carbon monoxide data supplemented by model output only approached critical levels just above flames in the most intense fires. By contrast, an ear-heating model driven by plume model output suggested that injury to the bat's thermally thin ears would occur up to heights similar to those of foliage necrosis, an effect for which predictive relationships exist. Risks of heat injury increase with fireline intensity and decrease with both roost height and ambient wind. Although more information is needed on bat arousal from torpor and behavior during fires, strategies for reducing the risk of heat injury emerge from consideration of the underlying causal processes.

**Résumé :** La mortalité de la faune et les blessures causées par les incendies de forêt constituent une préoccupation pour la gestion du feu et de la faune mais il existe peu de travaux portant sur les mécanismes associés aux effets d'une exposition. Dans cet article, nous utilisons un modèle intégral de panache, des mesures prises sur le terrain et des modèles des effets de la chaleur et du monoxyde de carbone pour explorer le risque que courent les chauves-souris qui se perchent dans les arbres lorsqu'on effectue des brûlages dirigés dans les forêts mélangées de chênes du sud-est de l'Ohio et de l'est du Kentucky. Les chauves-souris qui se perchent dans les arbres présentent un intérêt surtout parce que nous devons réduire les risques pour la chauve-souris de l'Indiana (*Myotis sodalis*), notre espèce cible, qui est menacée. La concentration de carboxyhémoglobine dans le sang prédite à partir de données de monoxyde de carbone complétées par les résultats d'un modèle ne fait que s'approcher des niveaux critiques exactement au-dessus des flammes des feux les plus intenses. Par contre, un modèle de réchauffement des oreilles alimenté par les résultats d'un modèle de panache indique que les oreilles thermosensibles des chauves-souris pourraient subir des dommages jusqu'à des hauteurs semblables à celles où se produisent des nécroses foliaires, un effet pour lequel il existe des relations prédictives. Les risques de dommages causés par la chaleur augmentent avec l'intensité de la ligne de feu et diminuent avec la hauteur à laquelle sont perchées les chauves-souris et les vents ambiants. Bien que davantage d'information soit nécessaire au sujet de la sortie de l'état de torpeur et du comportement des chauves-souris durant les incendies, des stratégies pour réduire les risques de dommages causés par la chaleur se dégagent de l'étude des processus causals sous-jacents.

[Traduit par la Rédaction]

## Introduction

Understanding and predicting the relatively direct effects of wildfires and prescribed fires on vegetation and fauna require consideration of both the behavior of fires (both flames and smoldering combustion) and the response of the organism of interest to the heat (Johnson and Miyaniishi

2001) and gas (Guelta and Balbach 2005; O'Brien et al. 2006) exposures that it experiences. Over decades, biophysical process models have been developed to predict the effects of flames and plumes on plants (e.g., Gill and Ashton 1968; Dickinson and Johnson 2001; Jones et al. 2006; Michaletz and Johnson 2006, 2007; Kavanagh et al. 2010) and soils (e.g., Aston and Gill 1976; Steward et al. 1990; Camp-

Received 2 January 2010. Accepted 30 July 2010. Published on the NRC Research Press Web site at cjfr.nrc.ca on 22 October 2010.

**M.B. Dickinson<sup>1</sup> and A.S. Bova.** US Forest Service, Northern Research Station, Forestry Sciences Laboratory, 359 Main Road, Delaware, OH 43015-8640, USA.

**J.C. Norris.** Norris Consulting Services, 6106 Worth Avenue, Benton, AR 72015, USA.

**R.L. Kremens.** Center for Imaging Science, Rochester Institute of Technology, 54 Lomb Memorial Drive, Rochester, NY 14623, USA.

**V. Young.** Department of Chemical and Biomolecular Engineering, Ohio University, 172 Stocker Center, Athens, OH 45701-2979, USA.

**M.J. Lacki.** Department of Forestry, University of Kentucky, Lexington, KY 40546, USA.

<sup>1</sup>Corresponding author (e-mail: mbdickinson@fs.fed.us).

bell et al. 1995). Yet, the mechanisms by which fauna are injured or killed during wildland fires have received insufficient attention even though faunal mortality in fires can be significant (Simons 1989; Esque et al. 2003). Of particular concern are threatened and endangered species that, despite possible evolution under regimes of frequent fire, may be vulnerable to mortality from fires (Gross 1923; Lunney et al. 2004; Engstrom 2010). The endangered Indiana bat (*Myotis sodalis*) is one such species that hibernates in caves and mines and, during the warmer months, resides in a broad range of eastern US habitats, including the extensive mixed-oak forests (USDI Fish and Wildlife Service 2007). In mixed-oak forests, burning has been practiced by humans for millennia for ecosystem management and other reasons. Today, prescribed fire is gaining acceptance as a means of restoring and perpetuating oak (*Quercus*) dominated ecosystems in the eastern United States (Nowacki and Abrams 2008). The Endangered Species Act requires that land management agencies work closely with the US Fish and Wildlife Service to minimize and mitigate adverse effects of habitat improvement projects and other activities on threatened and endangered species (e.g., USDI Fish and Wildlife Service 2007).

Because the Indiana bat is federally listed as endangered, and due to a lack of knowledge about its response to wildland fires, we need to better understand the risks for this bat so that land management practices can be developed that reduce risk while allowing the use of fire for oak ecosystem management and, potentially, bat habitat improvement (Dickinson et al. 2009). Indiana bats roost below bark and, to a lesser extent, in crevices in trees in mixed-oak forests, primarily selecting dead trees (snags) for roosting, particularly those that are larger than the average available and otherwise suitable snag (Lacki et al. 2009a). Simulations of gas and heat exchange into small-volume bark flap roosts showed that they offered little protection from exposure (Guelta and Balbach 2005 and unpublished data). Although large plates of sloughing bark may provide additional protection to roosting bats, we assumed that bats would be exposed to the full effects of the plume, i.e., they would be exposed to gases at a temperature, concentration, and velocity dependent only on smoke transport processes in the plume above a surface fire and not mitigated by sheltering effects.

Risk to juvenile (young-of-the-year) and adult bats may be particularly dependent on torpor, a diurnal hibernation-like state in which body temperatures track roost temperatures. Bats use torpor extensively for energy conservation outside of the hibernation period (e.g., Kurta 1991; Willis et al. 2006). The time to arousal from torpor (to a body temperature at which flying can occur) may take minutes to tens of minutes (see Discussion section) and shows a negative-exponential relationship with ambient temperature in bats and other small mammals that use torpor (e.g., Geiser 1986; Layne 2009). Male bats use torpor routinely, while females that are pregnant or nursing young may use torpor only when foraging conditions are poor, e.g., during cool and wet weather (Dickinson et al. 2009). Arousal may occur from a combination of olfactory and aural cues (Scesny and Robbins 2006). Neonatal bats that cannot fly and are too heavy to be carried by their mothers during flight likely

would be at greater risk to smoke effects than juveniles or adults (USDI Fish and Wildlife Service 2007). However, prescribed burning in the range of the Indiana bat would rarely be conducted in forests during the peak of summer when neonatal bats are present in tree roosts (Dickinson et al. 2009).

Carbon monoxide (CO), a major component of wildland fire smoke (e.g., Andreae and Merlet 2001; Wiedinmyer et al. 2006), causes buildup of carboxyhemoglobin (COHb) in blood and interferes with oxygen transport and exchange. At high concentrations, COHb leads to incapacitation and death. CO is expected to be the most significant toxicant in wildland fire smoke (Purser 1988). Irritants such as acrolein and formaldehyde are a class of combustion products that depress respiratory rates and reduce the volume of air inhaled with each breath. The product of the rate of respiration and the volume of air inhaled determines the respiratory minute volume (RMV) ( $L \cdot \text{min}^{-1}$ ). Irritants in smoke tend to mitigate risk from gas exposures because they depress RMV (Kane and Alarie 1977; Nielsen et al. 1984). Tissue burning is determined both by imposed heat flux from conduction, radiation, and convection and by the properties of the tissue being heated (e.g., Diller et al. 1991). In humans, sweating reduces tissue heating (Purser 1988); this mechanism is not available to bats. Hair reduces heat flux to and from the skin (Gates 1980), but bat ears and wing membranes often are nearly hairless and exposed when bats are roosting.

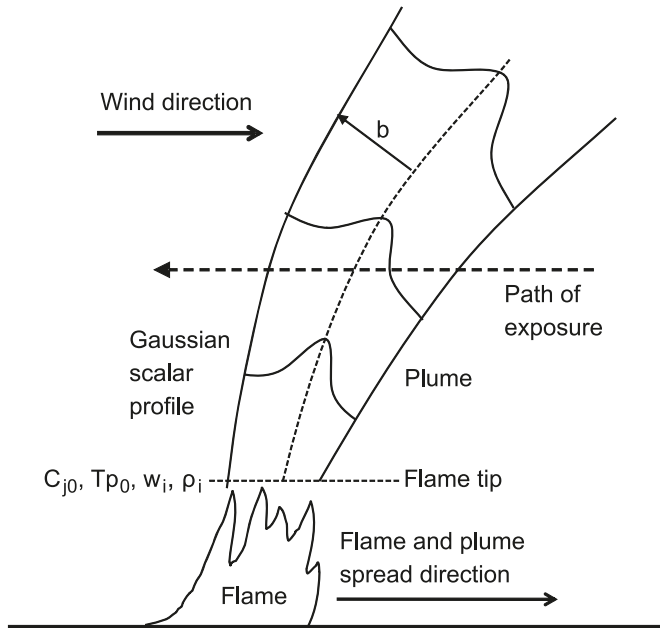
In this paper, we use COHb accumulation and tissue-burn models in conjunction with data on both fire and roosting behavior to explore risks to juvenile and adult tree-roosting bats from prescribed fires in mixed-oak forests. We report results from both field experiments, during which CO concentrations ( $[\text{CO}]$ ) were measured at 2.4 and 6.1 m (8 and 20 ft) above ground, and plume model simulations of  $[\text{CO}]$ , gas temperatures, and plume velocities and residence times. CO and associated irritant concentrations (acrolein and formaldehyde) were used as inputs to a COHb accumulation model and plume gas temperatures, velocities, and residence times were used as inputs to a tissue-burn model. Data from the plume model also were used to replace CO measurements when sensors saturated. Finally, we consider how risks to bats from prescribed fire might be mitigated.

## Methods and materials

### Modeled plume

An integral plume model was used to simulate gas concentrations and temperatures and their durations in a two-dimensional plume rising from a flame front (line source of heat) on flat terrain (Mercer and Weber 1994) (Fig. 1). The model requires solution of six coupled partial differential equations describing the conservation of mass, momentum, and energy. We included wind in our simulations because gas concentrations at a given height are expected to be reduced when there is ambient wind because of horizontal displacement and downwind distortion of the plume (e.g., Mercer and Weber 1994) (Fig. 1). When wind was applied, its velocity was constant with height. The coupled differential equations were solved with the Bulstoer function in

**Fig. 1.** A two-dimensional plume rising above a line fire in a crosswind. The wind comes from the left, causing plume deflection to the right. Flame spread also is to the right, causing objects in the canopy to experience a plume residence time that is a function of flame spread rate, wind velocity, and the object's height above ground. Flame conditions determine initial gas concentrations, temperatures, velocities, and densities. A Gaussian profile is fit to the top-hat (averaged) output of the plume model and used to calculate average plume properties. We do not consider deflection of the no-wind plume (not shown) in our model because flame spread is slow relative to plume velocity.



MathCad (Mathsoft 2001i; Professional, MathSoft Inc., Cambridge, Massachusetts).

To generate gases and heat, the model was run over a range of relevant fireline intensities (Byram 1959) prescribed by simultaneously increasing fuel loading and rate of spread (Table 1). Heat of combustion for convective heat release was constant at 16 000 kJ·kg<sup>-1</sup> (Nelson 2002). Boundary conditions for the plume model include initial flame velocity ( $w_i$ ), initial plume half-width ( $b_i$ ), flame tip (initial plume) temperature ( $T_{p0}$ ), and initial flame density ( $\rho_i$ ) (Table 1). Flame density (0.31 kg·m<sup>-3</sup>) was proportional to flame temperature (see below) from the ideal gas law. For this calculation, ambient air pressure at 500 m above sea level (Campbell and Norman 1998) was used to represent the region in which prescribed fires were monitored. Flame velocity was calculated from fireline intensity (kW·m<sup>-1</sup>) (Byram 1959) by Nelson's (2002) scaling relationship and plume half-width was one half of flame depth ( $D_f$ ) was calculated from

$$[1] \quad D_f = \frac{RW}{c}$$

where  $R$  is rate of spread (m·s<sup>-1</sup>),  $W$  is fuel consumption (kg·m<sup>-2</sup>), and  $c$  is combustion rate (kg·m<sup>-2</sup>·s<sup>-1</sup>) determined from experimental plot burns over a range of fuel consumption ranging from 0.3 to 3.4 kg·m<sup>-2</sup> (Bova and Dickinson

2008). The range in fuels loads used to estimate combustion rate spanned the range found in mixed-oak forests.

Products of combustion (POC) were assumed to mix immediately into a flame zone control volume defined in two dimensions by flame depth and length. The two-dimensional flame is analogous to the two-dimensional plume (Fig. 1). Flame length (equivalent to height in no-wind simulations) was calculated from fireline intensity as described by Weise and Biging (1996). The two-dimensional flux of a POC (kg·m<sup>-1</sup>·s<sup>-1</sup>) was determined from

$$[2] \quad \dot{m}_j = \frac{W_{2D}RY_j}{D_f}$$

where  $W_{2D}$  is two-dimensional loading (kg·m<sup>-1</sup>) and  $Y_j$  is yield of the POC (kg·kg<sup>-1</sup>). Yield estimates for biomass burning are taken from the literature (Table 2).

Gas concentrations in the flame control volume were calculated as

$$[3] \quad C_{fj} = \frac{n_j}{n_{CV}}$$

where  $C_{fj}$  is the concentration of POC  $j$ ,  $n_j$  is the number of moles of the POC, and  $n_{CV}$  is the number of moles of all gases in the control volume. The number of moles of a POC in the two-dimensional control volume is calculated as

$$[4] \quad n_j = \frac{\dot{m}_j(h_f D_f)^{\frac{1}{2}}}{M_j w_i}$$

where  $h_f$  is flame height (m) and  $M_j$  is the molecular mass of the POC (Table 2). The number of moles of all gases in the two-dimensional control volume is determined from the ideal gas law and ambient temperature:

$$[5] \quad n_{CV} = \frac{p_a(h_f D_f)^{\frac{1}{2}}}{R_{2D} T_f}$$

where  $p_a$  is ambient air pressure,  $R_{2D}$  is the gas constant for the two-dimensional control volume (8.314 m<sup>2</sup> Pa·K<sup>-1</sup>·mol<sup>-1</sup>), and  $T_f = 1000 + T_a$  (K) is the average temperature (above ambient,  $T_a$ ) of flames from biomass burning through their continuous and intermittent zones (Dupuy et al. 2003). Ambient temperature was set to 298 K.

Plume model output includes plume velocity, plume temperature, and concentrations of gas species at 1 m increments along the plume centerline. Because mixing is turbulent, we assume that mass and heat transfer rates between the plume and ambient air are similar. Thus, gas concentrations decline with height above the flame in proportion to declines in plume temperature:

$$[6] \quad C_{jh} = C_{fj} \left( 1 - \frac{T_{p0} - T_{ph}}{T_{p0} - T_a} \right)$$

where  $C_{jh}$  is concentration of POC  $j$  at height  $h$  above the flame,  $T_{p0} = 860 + T_a$  (K) is flame tip temperature above ambient (i.e., initial plume temperature; Dupuy et al. 2003), and  $T_{ph}$  is flame temperature at height  $h$  above the flame.

A Gaussian profile was fit to the top-hat results (Mercer and Weber 1994) and average gas concentrations, temperatures, and velocities over the residence time of the plume (i.e., travel time along the path of exposure from the leading

**Table 1.** Characteristics of fires used to generate boundary conditions for the plume model and the boundary conditions themselves.

$W$ (kg·m <sup>-2</sup> )	$R$ (m·min <sup>-1</sup> )	$I$ (kW·m <sup>-1</sup> )	$L_f$ (m)	$w_i$ (m·s <sup>-1</sup> )	$b_i$ (m)
0.5	1	133	0.7	1.9	0.10
1.0	2	533	1.4	3.1	0.42
1.5	3	1200	2.0	4.0	0.94
2.0	4	2133	2.6	4.9	1.68

**Note:** There is no interaction between wind and fire behavior in our model, only effects of wind on plume behavior and flame tilt (i.e., flame height) and thus the height above ground at which the plume begins. Fuel consumption ( $W$ ), rate of spread ( $R$ ), and heat of combustion determine fireline intensity ( $I$ ). Flame length ( $L_f$ ) and initial plume velocity ( $w_i$ ) are determined by  $I$  and initial plume half-width ( $b_i$ ) is determined by  $R$  and total and rate of fuel consumption.

**Table 2.** Yield and molecular masses of products of combustion from biomass burning.

POC	Yield (g·kg <sup>-1</sup> )	Molecular mass (g·mol <sup>-1</sup> )	Source
CO	94	28	Wiedinmyer et al. 2006
Acrolein	0.24	56	Andreae and Merlet 2001
Formaldehyde	2.2	106	Andreae and Merlet 2001
Water	609	18	Byram 1959

**Note:** CO yields are for deciduous forest fuels. Yield of water vapor is based on a fuel moisture content of 5% of dry mass, the fuel moisture content prescribed for plume simulations. Yields are used to calculate concentrations (see eqs. 2–6).

to trailing edge of the plume) (Fig. 1) were calculated horizontally across the plume at 1 m increments in height. Averaging in the horizontal over the residence times of plumes simulates exposures experienced by entities that do not move during the exposure, e.g., bats in roosts that are unable to flush during a fire. Flame heights were determined from fireline intensity as described in Weise and Biging (1996) and were used to normalize average plume characteristics to height above ground.

### Prescribed fire behavior and [CO]

Data on CO were obtained from four prescribed fires on dissected terrain in southeastern Ohio and eastern Kentucky. The Clark Hollow burn in Tar Hollow State Forest was conducted by the Ohio Department of Natural Resources, Division of Forestry, on 20 April 2007. Control lines were ignited by drip torch and the interior of the unit was ignited from a helicopter that dispensed delayed ignition devices (3.5 cm plastic spheres containing potassium permanganate injected with ethylene glycol just before they were dropped into the unit). Three additional burns were monitored on the Cumberland District of the Daniel Boone National Forest (DBNF). Conducted by DBNF staff, these burns were hand ignited with drip torches. Ignition at DBNF was along key control lines (e.g., roads, drainages) in combination with ridge ignition, i.e., where igniters walked ridges conducting point and line ignition. In ridge ignition, much of the area is burned by fires burning down slopes at low intensities. The Powder Mill burn was conducted on 10 April 2007, the Bear Waller burn on 30 April 2007, and the Wolf Pen burn on 8 April 2008. Neither the Powder Mill nor the Bear Waller unit had a history of prescribed burning; however, there are reports of “numerous fires having burned” within the original Cumberland purchase area before 1930 (Collins 1975, p. 195). The Wolf Pen unit is a frequently burned replicate of an ongoing research project on fire effects on vegetation and fuels (Loucks et al. 2008).

Towers were used to elevate instruments. Eco-Sense 2e electrochemical sensors from Sixth Sense, Inc., with a custom electronics signal conditioning board (that also measured sensor temperature) were placed at 2.4 and 6.1 m to monitor [CO] above fires. The heights chosen were standard for fire weather and meteorological measurements, respectively. The maximum [CO] that can be measured by these sensors is nominally 500 ppm. Eco-Sense electrochemical sensors are temperature compensated and respond linearly over the relevant concentration range (see sensor documentation at [www.citytech.com](http://www.citytech.com)). The sensors are not sensitive to orientation and were mounted on arms that extended 30 cm from the tower. We calibrated the sensor electronics package using 100 and 250 ppm calibration gases supplied by MESA Specialty Gases and Equipment (Santa Ana, California) to remove any variation due to the tolerances of custom electronic components. The background carrier in the calibration gas was nitrogen, which has no effect on the sensors. Sensors saturated below 500 ppm after this second calibration step (see Results).

A downward-facing, dual-band infrared radiometer with nominal view angle of 60° was positioned at 6.1 m on each tower and was used to measure fire radiative power (FRP) (kW·m<sup>-2</sup>) at a 5 s sampling interval. The instrument consists of two single-element thermopile detectors and amplifiers, filters, and power conditioners all mounted on a small circuit board. One detector (Perkin Elmer TPS 334) has a silicon long pass window that transmits from 5.5 to 15 µm, while the other detector (Dexter Research 2M) has a CaF<sub>2</sub> window with transmission from 0.2 to 9 µm. One of the thermopiles (TPS 334) has an integral thermistor to monitor and correct for the effects of finite sensor temperature. The instrument was calibrated using several Omega Corporation blackbody reference sources spanning temperature ranges from 373 to 1300 K. The process by which estimates of FRP were derived from dual-band data is described in Kremens et al. (2010).

All towers were placed in interior locations within burn units except for one tower at Tar Hollow inadvertently placed ~20 m from a control line. Towers were located in landscape positions that we anticipated would have a high probability of burning during the fires and, accordingly, tended to be on ridges and slopes with a southerly aspect where one would expect to encounter relatively dry fuels. Because all units also had areas with northerly exposures, the fire intensities and rates of spread and thus [CO] that we report would be expected to be above average for the units as a whole.

Modeled values used to replace saturated values were the average [CO] calculated from the plume model for the appropriate height and for the fireline intensity, ambient temperature, and wind speed matching those estimated for the tower and sensor from which the saturated measurement was obtained. Ambient temperature and wind at 6.1 m were averaged for the 10 min preceding fire arrival, as indicated by an initial increase in [CO]. Estimates of fireline intensity were derived from data from a set of fire behavior experiments in mixed-oak fuels described by Bova and Dickinson (2008). Peak FRP ( $\text{kW}\cdot\text{m}^{-2}$ ) was proportional to fireline intensity ( $I$ ) in these experiments:

$$[7] \quad I = 43.78\text{FRP}^{0.89}$$

where fireline intensity was estimated using measured rates of spread and fuel consumption and a heat of combustion of  $18\,700 \text{ kW}\cdot\text{m}^{-1}$  intended to describe both convective (flaming) and smoldering heat release (Johnson 1992) ( $R^2 = 0.73$ ). Equation 7 was used to estimate fireline intensity from peak FRP measured by the dual-band radiometer attached to each tower. Next, plume model average [CO] output from the simulations described in Table 1 was related to fireline intensity, ambient wind, and height above ground through a relationship describing temperature rise (excess) above ambient. Temperature excess ( $\theta = T_{p_h} - T_a$ , where  $T_a$  was set to  $25^\circ\text{C}$ , the average ambient temperature observed in the prescribed fires) at height in the plume was described for a line-source plume by Van Wagner (1973):

$$[8] \quad \theta \propto \frac{0.239I^2}{z_g(0.026I + U^3)^{1/2}}$$

where  $z_g$  is height above ground (m) and  $U$  is wind speed ( $\text{m}\cdot\text{s}^{-1}$ ) and conversion factors and coefficients are combined. Fireline intensities for the plume model (Table 1) were based on a heat of combustion for convective heat release alone ( $16\,000 \text{ kW}\cdot\text{m}^{-1}$ ) and were adjusted upward to  $18\,700 \text{ kW}\cdot\text{m}^{-1}$  for use in eq. 8 (see eq. 7). Finally, model [CO] values at height were described by a combination of eq. 8 and an added group of variables to obtain the best fit to model output (see Results).

To further describe prescribed fire behavior, fuel consumption was estimated from fire radiative energy ( $\text{kJ}\cdot\text{m}^{-2}$ ), the time integral of FRP, using the proportionality estimated by Wooster et al. (2005). We have validated Wooster et al.'s (2005) relationship for mixed-oak fuels using data from the experiments described in Bova and Dickinson (2008) and calculations described in Kremens et al. (2010).

## Modeling incapacitation from prescribed fire CO exposures

Incapacitation from smoke exposures was modeled from the combined and counteracting effects of CO and irritant exposures on COHb concentrations (%) in the blood. We assumed that COHb accumulation from CO exposures in bats was similar to that for rats, an assumption supported by the similarity in dose–response relationships seen across a wide range of taxa and body masses (e.g., Speitel 1996). Accumulation of COHb was modeled for field CO exposure data through a relationship developed by Hartzell et al. (1985) on the basis of data from rats. This relationship was applied to each time step and the effects of sequential time steps summed to provide a cumulative COHb concentration at the end of an exposure as

$$[9] \quad \text{COHb} = \sum_{j=1}^n [12.5 \ln([\text{CO}]_j) - 22.9] [1 - e^{(-kt[\text{CO}]_{\text{RMV}})_j}]$$

where the summation occurs from time step  $j = 1$  to  $n$ ,  $k$  is the time constant ( $4.057 \times 10^{-4} \cdot \text{min}^{-1}$ ), and  $t$  is the time step (0.17 min). We applied eq. 9 to the main exposure period (when flames were passing below towers), ending COHb accumulation once [CO] had fallen toward background levels characteristic of post-fire residual combustion and the COHb dissociation process would be expected to result in a relatively rapid (~30 min half-life) decline in COHb concentrations (e.g., Kim et al. 1991).

To determine a lower threshold [CO] to include in COHb accumulation calculations and to serve as an initiation value for COHb dissociation, we used the rule of thumb that human hemoglobin affinity for CO is  $\geq 200$  times that for  $\text{O}_2$  (Ernst and Zibrak 1998). In the plume model,  $\text{O}_2$  was 200 times more abundant than CO and thus was competitive with CO for binding with hemoglobin when [CO] values were ~100 ppm. Thus, only [CO] values  $\geq 100$  ppm were included in the summation in eq. 9.

Data on time-to-incapacitation for rats as a function of [CO] from Kaplan and Hartzell (1984) were used in eq. 9 to calculate the COHb concentration associated with incapacitation. The results suggest that COHb concentrations required to induce incapacitation range from 70% to 93%. To provide a margin of safety, a threshold value for incapacitation of 50% COHb was chosen for assessing the potential effects of prescribed fire smoke exposures. Data for humans suggest greater sensitivity to COHb, with loss of consciousness predicted at 40% or lower and death at 50% or higher (Purser 1988).

In our analysis, we assumed that the affinity of bat hemoglobin for CO was similar to that for rat hemoglobin. The basis for this assumption was the similarity of the  $P_{50}$  values for rodent hemoglobin versus bat hemoglobin. The  $P_{50}$  value is the  $\text{O}_2$  partial pressure at which 50% of the hemoglobin is saturated with  $\text{O}_2$ . Thus, it is an indication of the hemoglobin affinity for  $\text{O}_2$ ; a lower  $P_{50}$  value means a higher affinity of hemoglobin for  $\text{O}_2$ . The  $P_{50}$  value for *Phyllostomus discolor* was 28.6 Torr, while the  $P_{50}$  value for two other bats, *Rousettus aegyptiacus* and *Myotis myotis*, was 30.8 and 33.3 Torr, respectively (Jürgens et al. 1981). Conversely, the  $P_{50}$  value for white mice and white rats has been reported to be 42 and 36 Torr, respectively (Lahiri 1975). Another reported

$P_{50}$  value was 44 Torr for the laboratory mouse, which was similar to *Phyllostomus discolor* in size (Schmidt-Neilsen and Larimer 1958). Wild-caught mice, *Clethrionomys glareolus* and *Apodemus sylvaticus*, had  $P_{50}$  values of 33.2 and 33.5 Torr, respectively (Jürgens et al. 1981).

Effects of irritants in smoke were incorporated because they reduce RMV. Resting RMV averaged 0.021 L·min<sup>-1</sup> for the rats in Hartzell et al. (1985). Estimated RMV for a 15 g big brown bat (*Eptesicus fuscus*) at 37 °C was 0.023 L·min<sup>-1</sup> (Szewczak and Jackson 1992), and Chappell and Roverud (1990) reported an RMV of 0.023 L·min<sup>-1</sup> at 37 °C for *Noctilio albiventris* (mean mass 40 g). Accordingly, we used an RMV of 0.023 L·min<sup>-1</sup> as the base value in our assessments of COHb accumulation. We assume that RMV is the basal rate even though bat metabolic and breathing rates during torpor are lower than those at the basal body temperature (37 °C) and increase with body temperature during the torpor arousal process (Hayward and Ball 1966). Our assumption of a basal RMV would tend to overestimate COHb accumulation.

Acrolein and formaldehyde were selected for analyses on the basis of their prominence among forest fuel combustion products and their known effects on RMV. Equations relating formaldehyde and acrolein mole fractions (ppm) to percent decrease in respiration rate (breaths·min<sup>-1</sup>) were determined by nonlinear least squares regression on data from the literature. Under an assumption of a constant tidal volume (L), a decrease in respiration rate translates directly into a decrease in RMV. For mice, percent decrease in respiration rate as a function of formaldehyde concentration [CH<sub>2</sub>O] is based on data from Chang et al. (1981):

$$[10] \quad \% \text{ decrease} = \frac{72.57[\text{CH}_2\text{O}]}{1.96 + [\text{CH}_2\text{O}]}$$

collected over the concentration range of 0.8–15 ppm. For mice, the relationship describing percent decrease in respiration rate as a function of acrolein concentration [C<sub>3</sub>H<sub>4</sub>O] is based on data from Nielsen et al. (1984):

$$[11] \quad \% \text{ decrease} = \frac{89.96[\text{C}_3\text{H}_4\text{O}]}{2.09 + [\text{C}_3\text{H}_4\text{O}]}$$

collected over the concentration range of 0.4–7.3 ppm. The irritancy of the bats was assumed to be the same as that for mice for both acrolein and formaldehyde. We assume that the effects of these irritants are additive (Cassee et al. 1996) so the percent decrease in respiration rates for acrolein and formaldehyde was added in the equation for the calculation of COHb concentrations. Acrolein is a somewhat more potent irritant with an RD<sub>50</sub> value (irritant concentration at which there is a 50% decrease in respiration rate) of 1.7 ppm after 10 min exposures to a range of concentrations compared with formaldehyde with an RD<sub>50</sub> value of 3.1 ppm after 10 min exposures (Kane and Alarie 1977). It was determined that the concentrations of irritants were below lethal levels given the relatively short exposure times for these gases. As a result, only the irritants' effects on breathing rates were considered.

To get a sense of the rate of COHb dissociation and CO elimination and identify where exposures could be said to end, we initiated dissociation when measured [CO] fell be-

low 100 ppm. We estimated the time constant for dissociation from data in Kim et al. (1991):

$$[12] \quad \text{COHb}_{(t+1)} = \text{COHb}_{(t=0)}e^{-lt}$$

where COHb<sub>(t+1)</sub> is COHb concentration at the end of the time step, COHb<sub>(t=0)</sub> is COHb concentration at the beginning of the time step,  $l$  is the time constant (0.0003·s<sup>-1</sup>), and  $t$  is our 10 s sampling interval. In Kim et al.'s (1991) data set, rats were exposed to 3700 ppm CO for 30 min and COHb concentrations were >50%.

### Modeling burns caused by elevated plume temperatures

Because we had no data on plume gas temperatures from the prescribed fires, plume model data were used to assess risk from exposures to elevated temperatures. We modeled thermal effects on bats by considering the heating of bat ears. These thermally thin appendages are exposed when bats are roosting in their typical head-down position. We chose this approach because there are no models or data specific to bats regarding thermal effects and no appropriate models or data available for other small mammals. We do not believe that models or databases on human exposures (e.g., Blockley 1965) are appropriate given the differences in thermal mass between human and bat appendages and the ability of humans to use sweating as a heat sink.

If an object can be assumed to exhibit a small temperature gradient from its surface to its interior during heating, a simplified lumped-capacitance approach can be applied (e.g., see derivation in Holman 1986). The lumped-capacitance model has been applied to predicting the heating of small buds and twigs (e.g., Michaletz and Johnson 2006) and cones (Gutsell and Johnson 1996) in wildland fires. The criterion for applying the model is the Biot number (Bi):

$$[13] \quad \text{Bi} = \frac{cV}{h}$$

where  $c$  is the heat capacity of the material (J·kg<sup>-1</sup>·°C<sup>-1</sup>),  $V$  is the volume (kg·m<sup>-3</sup>), and  $h$  is the convection heat transfer coefficient (W·m<sup>-2</sup>·°C<sup>-1</sup>). The Biot number provides a ratio of internal resistance to heating to potential convective heat flux. Internal temperature gradients can be assumed to be small enough to ignore when Bi < 0.1. The ears of the Indiana bat are nearly hairless. Ear skin thickness in *Myotis septentrionalis*, a species with similar body size and hairless ears of similar morphology, was 0.16 mm ( $N = 3$  bats). As a first approximation for calculations of convective heat transfer coefficients, we assume that the head of a roosting bat is approximately spherical in shape. The average convection heat transfer coefficient for a sphere is a function of head dimension and gas temperature and flow rate and can be estimated by solving the following relationships for  $h$  (Gates 1980):

$$[14] \quad \text{Nu} = 0.37\text{Re}^{0.6}$$

$$[15] \quad \text{Nu} = \frac{hD}{k}$$

$$[16] \quad \text{Re} = \frac{VD}{\nu}$$

where  $Nu$  is the Nusselt number (dimensionless),  $Re$  is the Reynolds number (dimensionless),  $D$  is the diameter of the bat's head (15 mm for the Indiana bat) (NatureServe 2009),  $k$  is air thermal conductivity ( $\text{W}\cdot\text{m}^{-1}\cdot\text{C}^{-1}$ ),  $\nu$  is the kinematic viscosity of air ( $\text{m}^2\cdot\text{s}^{-1}$ ), and  $V$  is plume velocity ( $\text{m}\cdot\text{s}^{-1}$ ). Air thermal conductivity and kinematic viscosity are dependent on plume gas temperature and were calculated from Sutherland's formula (Rogers 1992) assuming a constant heat capacity of air of  $1030 \text{ J}\cdot\text{kg}^{-1}\cdot\text{K}^{-1}$  (at 500 K). As with CO exposures, we assume that the roosting bat experiences the full temperature and velocity of the plume with no sheltering.

The lumped-capacitance model can be arranged to provide the time to burn injury:

$$[17] \quad t_N = \ln \theta_N \left( \frac{\rho c V}{hA} \right)$$

where  $t_N$  is time to necrosis (s),  $\theta_N$  is the temperature excess at necrosis ( $(T_N - T_{p_h}) / (T_a - T_{p_h})$ , where  $T_N$  is set to  $60 \text{ }^\circ\text{C}$  and  $T_a$  to  $25 \text{ }^\circ\text{C}$ ),  $\rho$  is density of the skin ( $1040 \text{ kg}\cdot\text{m}^{-3}$ ; Diller et al. 1991),  $c$  is skin heat capacity ( $4000 \text{ J}\cdot\text{kg}^{-1}\cdot\text{C}^{-1}$ , Diller et al. 1991), and  $V$  and  $A$  are volume and area, respectively, of a  $1 \text{ cm} \times 1 \text{ cm}$  patch of skin. Residence time required for necrosis was compared with plume residence times to determine the heights in the plume up to which burn injury was expected.

## Results

### Plume model output

General relationships between modeled plume characteristics, height above ground, and fireline intensity for no-wind plumes are shown in Fig. 2. CO concentrations and gas temperatures increased with fireline intensity yet both declined sharply with height as the plume mixed with ambient air. Plume velocities accelerated above the flame but were nearly constant thereafter, the lack of continued acceleration reflecting the reduction in buoyancy with mixing. Crosswinds caused plume distortion from the no-wind case and led to lower temperatures and [CO] at a given height (Fig. 1).

Initial plume residence times were determined by flame rate of spread and flame residence time and increased with height above ground as the plume expanded, particularly at low fireline intensities where flame rates of spread and plume velocities were lowest. For no-wind fires (Fig. 2d), the range was 15 s near the flame tip (0.7 m above ground) for the fire with the lowest fireline intensity ( $133 \text{ kW}\cdot\text{m}^{-1}$ ) to as long as 10 min for the same fire at 31 m above ground. Residence times for fires of higher fireline intensity fell within that range over all heights. For fires burning in a  $2 \text{ m}\cdot\text{s}^{-1}$  crosswind, the range in residence times was 1 min for the fire with the highest fireline intensity ( $2133 \text{ kW}\cdot\text{m}^{-1}$ ) near the flame tip (3.6 m) and 78 min at a height of 31 m for the same fire. Residence times for the  $1 \text{ m}\cdot\text{s}^{-1}$  crosswind were intermediate between the no-wind and  $2 \text{ m}\cdot\text{s}^{-1}$  simulations. Results for low-intensity fires in crosswinds are not reliable because of plume distortion (Van Wagner 1973), particularly for predictions high into the canopy. However, plume model [CO] values were toxicologically significant only for high-intensity fires where sensor saturation occurred

and for heights below which plume temperatures and velocities were sufficient to cause ear injury (see below).

Plume model average [CO] values from simulations described in Table 1 were related to fireline intensity, ambient wind, and height above ground for use in correcting for sensor saturation where that occurred (Table 1). Equation 8, which describes temperature excess  $\theta$ , was used along with an added group of variables to tailor the relationship to [CO]:

$$[18] \quad [\text{CO}] = 59.8 \left\{ \frac{\theta}{[(U+1)z_g]^{1/3}} \right\}$$

where the denominator was chosen for best fit ( $R^2 = 0.98$ ). Equation 18 was used to replace saturated values by mean modeled [CO] ranging from 484 to 1,817 ppm for sensors at a height of 2.4 m and from 377 to 1,650 ppm for sensors at a height of 6.1 m. Model values at 6.1 m for several low-intensity fires were less than saturated values and in this situation saturated values were not replaced. Concentrations of formaldehyde and acrolein estimated from emission factors in Table 2 were  $<2.6$  ppm for formaldehyde and  $<0.2$  ppm for acrolein for [CO] up to 2,000 ppm.

### Prescribed fires

General prescribed fire conditions are summarized in Table 3 and conditions at each tower are summarized in Table 4. Three to five monitoring towers were deployed in each fire. Fireline intensities estimated from peak FRP ranged from 90 to  $894 \text{ kW}\cdot\text{m}^{-1}$ . Fuel consumption estimated from integrated fire radiative energy ranged from 0.13 to  $1.56 \text{ kg}\cdot\text{m}^{-2}$ . Ambient temperatures when fires burned by towers averaged from 18 to  $33 \text{ }^\circ\text{C}$ . Relative humidities from nearby fire weather stations (remote automated weather stations) ranged from 21% to 45%. Measured peak [CO] and, where saturated, modeled average [CO] are given. Saturation values ranged from 334 to 436 ppm. In general, CO exposures near the ground (2.4 m) are higher than at 6.1 m, as expected from the plume model.

Time courses of [CO] are provided for fires with the highest, near median, and lowest fireline intensities as a means of illustrating the range in exposures (Fig. 3). The rapid rise and saturation of sensors in the highest intensity fires along with a long period of residual combustion and smoke transport from beyond the immediate area of the tower is illustrated for the Powder Mill tower in Fig. 3a. A gradual rise and fall of exposures (Fig. 3) resulted from relatively weak plumes. COHb accumulates most rapidly where [CO] is highest, and, as described in the Methods and materials section, when [CO]  $< 100$  ppm, only COHb dissociation occurs.

### Incapacitation from CO

Modeled COHb concentrations approached the 50% threshold only at 2.4 m above ground at two towers (Table 4). The towers in question experienced the most intense burning. For all towers, modeled COHb values were lower at 6.1 m than at 2.4 m except in one case for which values were equal at the two heights. There was a general positive relationship between fireline intensity and modeled COHb (Table 4).

Modeled COHb is used as the basis for comparison be-

**Fig. 2.** No-wind plume characteristics predicted from the integral model. (a) CO concentration, (b) gas temperatures, (c) plume velocities, and (d) residence times are shown as a function of height above ground and fireline intensity (see Table 1). Note that the orientation of axes changes among plots.

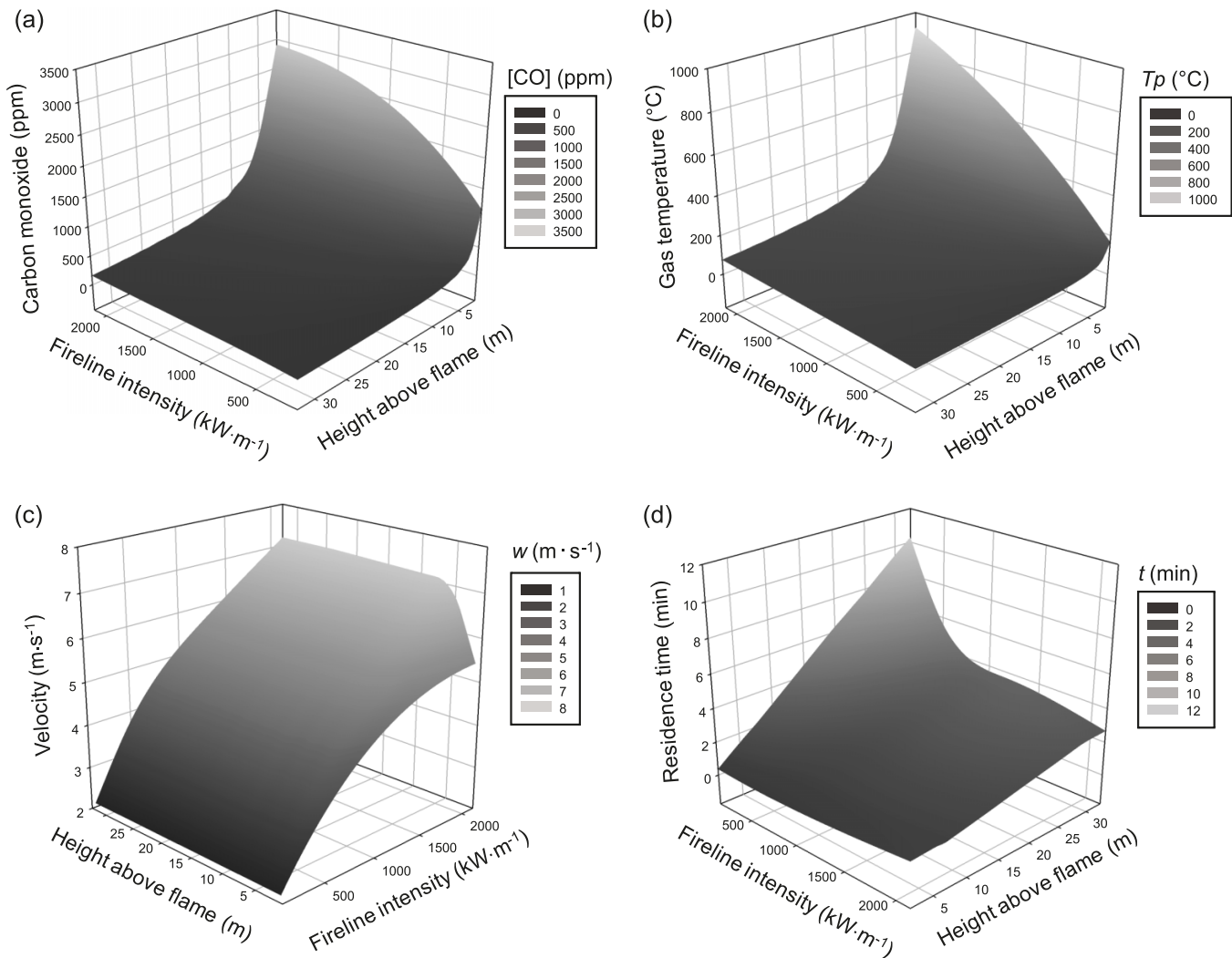


**Table 3.** General characteristics of prescribed fires in southeastern Ohio and eastern Kentucky.

Burn unit	Date	State	RAWS	Area (ha)	$T_a$ (°C)	Relative humidity (%)	$U$ (m·s <sup>-1</sup> )
Powder Mill	10 April 2007	Kentucky	Koomer	425	18.5	21	0.43
Tar Hollow	20 April 2007	Ohio	Zaleski	132	22.5	31	0.70
Bear Waller	30 April 2007	Kentucky	Koomer	176	32.0	26	0.40
Wolf Pen	8 April 2008	Kentucky	Triangle	117	26.0	45	

**Note:** Averages across towers at 6.1 m are provided for temperature and wind speed except for Wolf Pen where temperature is from the nearest fire weather station (remote automated weather station (RAWS)). Values for relative humidity are the midafternoon value (15:00) from the nearest RAWS except for Tar Hollow for which the Zaleski RAWS was more representative. Data specific to individual towers are provided in Table 4. All fires in Kentucky were on the Cumberland District of the Daniel Boone National Forest. The unit size is larger than the area burned, particularly for fires in the Daniel Boone National Forest where ridge ignition was practiced. The Tar Hollow burn was ignited by hand and helicopter.

tween plume model and field CO exposures (Fig. 4). Modeled COHb is plotted against Van Wagner's (1973) temperature excess variable (eq. 8), which provides a reasonable description of variability in the data. The highest COHb estimates from the prescribed fire CO exposures are more than twice as high as those resulting from plume model exposures. Because [CO] values are higher in the plume model output than in the data sets derived from the field data, we conclude that short plume residence times (Fig. 2d) are the

cause of low blood COHb concentrations predicted from the plume model output.

#### Gas temperature effects

Biot numbers were always  $\leq 0.08$ , so we used the lumped-capacitance model to assess ear injury. Figure 5 shows the heights above ground up to which bat ear burns would be predicted to occur for fires of increasing fireline intensity burning under a range of ambient wind velocities. For a

**Table 4.** Characteristics of prescribed fires at towers in mixed-oak forests of southeastern Ohio and eastern Kentucky.

Fire	Behavior	Fire radiative power (kW·m <sup>-2</sup> )	Fire radiative energy (kJ·m <sup>-2</sup> )	<i>I</i> (kW·m <sup>-1</sup> )	<i>W</i> (kg·m <sup>-2</sup> )	<i>U</i> (m·s <sup>-1</sup> )	<i>T<sub>a</sub></i> (°C)	Maximum [CO] (ppm)		COHb (%)	
								Height 6.1 m	Height 2.4 m	Height 6.1 m	Height 2.4 m
Powder Mill	Heading uphill	29.1	3770	894	1.39	0.4	18	524 <sup>a</sup>	1817 <sup>a</sup>	—	45
Bear Waller		21.6	875	685	0.32	—	—	—	—	—	—
Bear Waller		19.5	4231	623	1.56	0.4	32	407 <sup>a</sup>	1410 <sup>a</sup>	16	43
Tar Hollow	Flanking across slope	17.3	3806	562	1.40	0.5	22	377 <sup>a</sup>	1308 <sup>a</sup>	7	25
Tar Hollow	Heading across slope	12.5	1563	418	0.58	0.7	23	205	1013 <sup>a</sup>	1	13
Powder Mill		8.9	1661	308	0.61	0.4	19	367 <sup>b</sup>	883 <sup>a</sup>	3	11
Powder Mill	Flanking downhill	5.4	1922	198	0.71	0.5	—	297	—	2	—
Tar Hollow	Backing downhill	3.4	1128	130	0.41	0.5	23	243	264	1	2
Bear Waller		3.2	925	125	0.34	0.4	33	353 <sup>b</sup>	484 <sup>a</sup>	4	16
Powder Mill		3.2	2886	122	1.06	—	—	—	—	—	—
Wolf Pen	Backing downhill	3.0	1670	117	0.61	—	—	115	212	0	1
Tar Hollow	Flanking across slope	2.7	1594	107	0.59	1.1	22	375	335 <sup>b</sup>	4	4
Bear Waller	Heading uphill	2.4	1811	97	0.67	0.4	31	360	436 <sup>b</sup>	4	5
Wolf Pen		2.4	1745	95	0.64	—	—	158	313	1	6
Wolf Pen		2.3	362	91	0.13	—	—	103	214	0	1
Wolf Pen	Backing downhill	2.2	1384	90	0.51	—	—	5	179	0	2

**Note:** The table is sorted by peak fire radiative power. Towers were placed in landscape positions that were expected to burn, so are not representative of burn unit averages. Ambient temperatures ( $T_a$ ) and winds ( $U$ ) were estimated for the 10 min preceding fire arrival. General fire behavior below towers was determined from video (where available), with heading, flanking, and backing referring to fires burning with the wind, perpendicular to the wind, and against the wind, respectively, and uphill, across slope, and downhill referring to fire spread direction relative to the prevailing slope. Maximum measured [CO] values are provided for the two sensor heights except where sensor saturation occurred. For saturated values, the average [CO] from the plume model that was used to replace saturated measurements is given. Partial or complete sensor system failures are indicated by dashes. Modeled COHb concentrations were derived from the time course of measured and, where saturated, modeled [CO].

<sup>a</sup>The saturated [CO] measurement is replaced by model average [CO].

<sup>b</sup>The modeled average [CO] value was lower than the saturated [CO] measurement; thus, the measured maximum value is given.

**Fig. 3.** Representative CO exposures and blood COHb concentrations from prescribed fires in southeastern Ohio and eastern Kentucky ((a) Powder Mill, (b) Tar Hollow, and (c) Wolf Pen). Shown are the time courses of CO exposures at 6.1 m (top) and 2.4 m (bottom) above ground. Data are from towers that captured the highest, near median, and lowest median fireline intensities (see Table 3). Saturated [CO] values were replaced by model average values (see Methods and materials section). The CO sensor saturation limits are indicated for the Powder Mill tower by arrows. COHb accumulation is calculated where no sensor failure occurred (e.g., Fig. 3a at 6.1 m) and where [CO] rises above 100 ppm. Note that the vertical scales change among figures.

given fireline intensity, crosswinds tended to decrease the heights at which ear burns would occur. As fireline intensity increased, the modeled height at which ear injury was predicted increased linearly over the range of interest. Average and minimum roost heights recorded for Indiana bats along with the range of fireline intensities observed at towers within the prescribed fires are shown in Fig. 5. Under our model scenarios, with bats being exposed in roosts to the full effect of the plume, ear injury often would be predicted at the mean roost height at fireline intensities typical of prescribed fires. The height of ear injury corresponded approximately to the height at which 60 °C was reached in the plume (eq. 17).

## Discussion

On the basis of prescribed fire CO exposures and modeled COHb concentrations, CO toxicity for tree-roosting bats, e.g., the Indiana bat, that are exposed to the plume is unlikely to be a concern at fireline intensities below 900 kW·m<sup>-1</sup> (~1.6 m flame length) (Table 4). Because of short residence times, our plume model CO exposures led to even lower predicted COHb concentrations than those determined for the field data (Fig. 4). Higher fireline intensities than those that we observed at our towers in four prescribed fires (Table 4) occur during prescribed burning in our region, but attempts often are made to avoid high intensities because of the injury they cause to trees. In contrast with CO effects, our results suggest that Indiana bats often would be vulnerable to ear burns under typical prescribed fire conditions because of their head-down roosting orientation and fine ear structure (Fig. 5). As a rule of thumb, bat injury would be expected at the same height as foliage necrosis, which has been described as the height at which 60 °C is reached in the plume (Van Wagner 1973). The 60 °C rule of thumb for ear injury results from both our chosen necrosis temperature (60 °C) and the short residence times required to cause necrosis of thermally thin ear tissue (eq. 17).

The risk to tree-roosting bats is contingent on their presence in forests during periods when burns are being conducted and, if present, their ability to fly to escape heat and gases. A review of dates at which Indiana bats emerge from hibernation and begin using forest habitats shows that females tend to emerge earlier than males (USDI Fish and Wildlife Service 2007). Depending on weather and climate, peak emergence for females ranged from early to mid-April and peak emergence for males ranged from the end of April to early May (e.g., Hall 1962; Cope and Humphrey 1977). Emergence began as early as late March (e.g., Hall 1962; Hobson and Holland 1995). In the fall, males are active for longer than females (e.g., Cope and Humphrey 1977). Most bats observed in Kentucky, Indiana, and Illinois had entered hibernation by the end of November (Hall 1962), while most

bats had entered hibernation by mid-October in a more northerly hibernaculum (Kurta et al. 1996). Indiana bat populations at some hibernacula may increase throughout fall and into January (Clawson et al. 1980), while numbers decline through the winter in others (Hall 1962). Currently, most prescribed fires in the central hardwoods region are conducted during the late winter and early spring. For most national forests, burns are not conducted past the end of April (Dickinson et al. 2009). Clearly, only the earliest burns in the spring and latest burns in the fall would occur when no bats were in forests.

The vulnerability of adult bats to smoke outside of the hibernation period is contingent on torpor dynamics, about which too little is known to make reliable assessments. Key issues are the cues that initiate arousal for a given species, the time required for flight once the arousal process begins, and the gender differences in torpor behavior during the burning season (reviewed in Dickinson et al. 2009). Information on arousal cues and times for eastern red bats (*Lasiurus borealis*) (Scesny 2006; Scesny and Robbins 2006; Layne 2009) provides useful guidance but confirmation is required for other tree-roosting species. Because eastern red bats hibernate in the leaf litter during cold periods, their populations may have experienced greater selective pressures for smoke sensitivity. In any case, they have been observed to flush in front of fires (Moorman et al. 1999). Additional information is needed on bat torpor, arousal, and flushing during prescribed burning. Currently, only Dickinson et al. (2009) have investigated the behavior of bats fitted with transmitters and, then, only in a single prescribed fire.

Because of reduced sheltering, bats roosting in foliage would be expected to be as or more vulnerable to smoke effects than Indiana bats that show a preference for roosting below sloughing bark (e.g., Lacki et al. 2009a). Bats known to roost in foliage include eastern red bats, hoary bats (*Lasiurus cinereus*), and silver-haired bats (*Lasionycteris noctivagans*) (NatureServe 2009). Bats that preferentially roost in crevices (e.g., the northern bat (*Myotis septentrionalis*); Lacki et al. 2009a) and cavities (Rafinesque's big-eared bats (*Corynorhinus rafinesquii*); Gooding and Langford 2004) may be somewhat less vulnerable to smoke effects than other tree-roosting bats because of the reduced rates of gas mixing into cavities (Guelta and Balbach 2005 and unpublished data).

Eastern red bats have been shown to use both the sound and smell of fires as cues for arousal (Scesny 2006). These bats hibernate in the leaf litter during cold periods in oak forests where fires were frequent historically. In Scesny (2006), bats were aroused from smoke exposure alone and, more rapidly, from the combination of smoke and playback of sound recordings of fire. They were not aroused from the sound of fire alone. Absent additional data, we must assume that the response of tree-roosting bats such as the Indiana bat to fire cues is similar to that of eastern red bats.

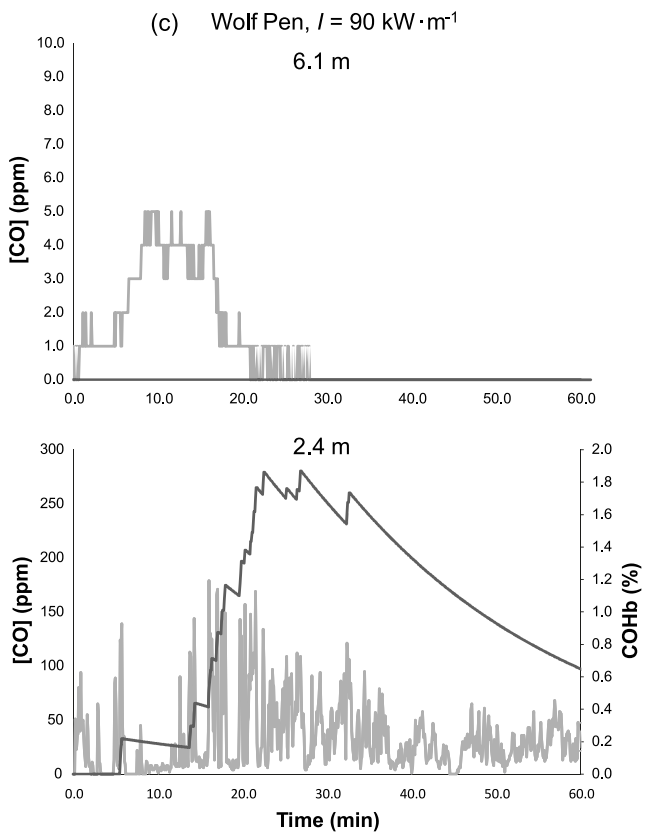
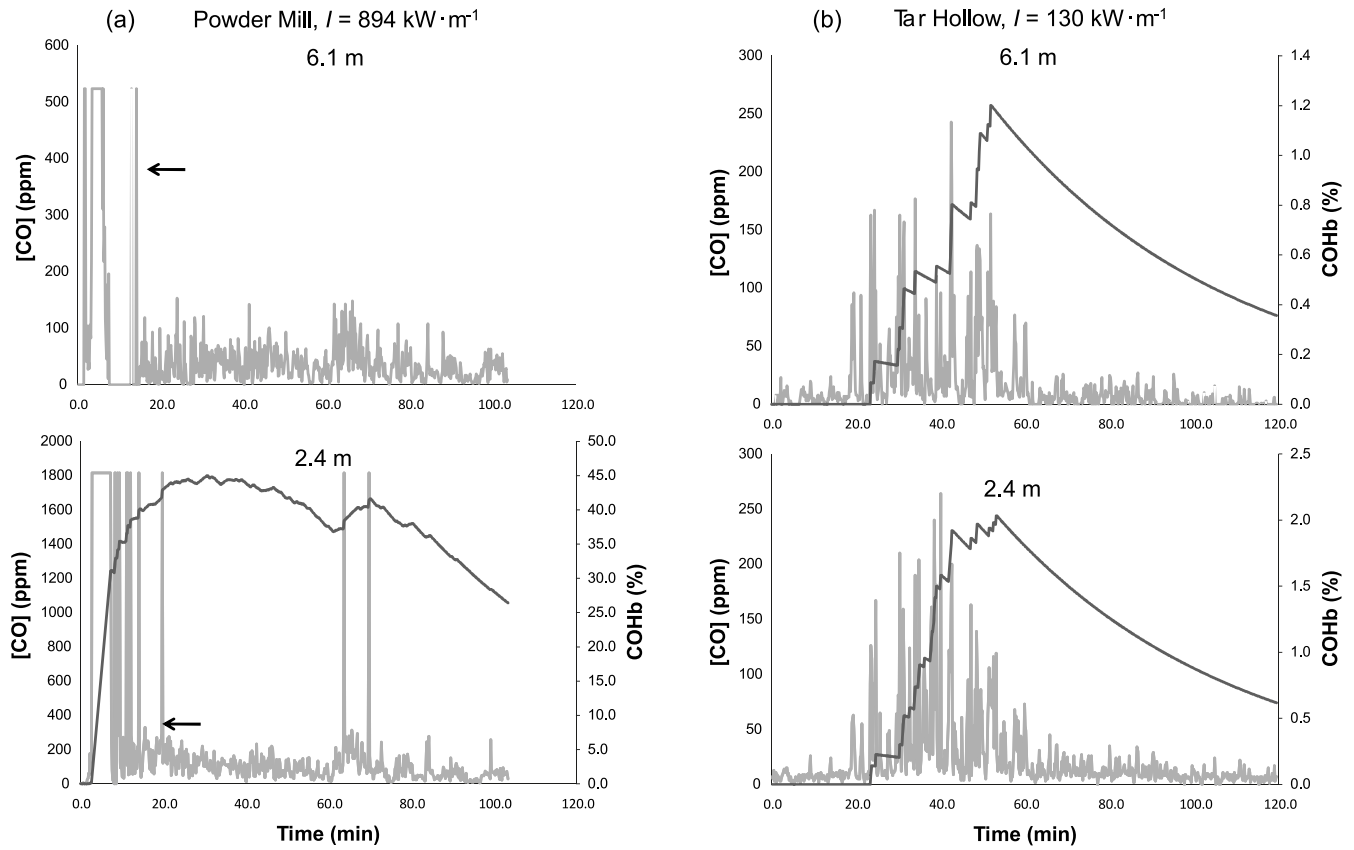


**Fig. 4.** Comparison of predicted blood COHb between prescribed fires (open diamonds) and plume model runs (solid diamonds). By capturing functional relationships among explanatory variables, the temperature excess variable (eq. 9) reduces variability in the relationships.

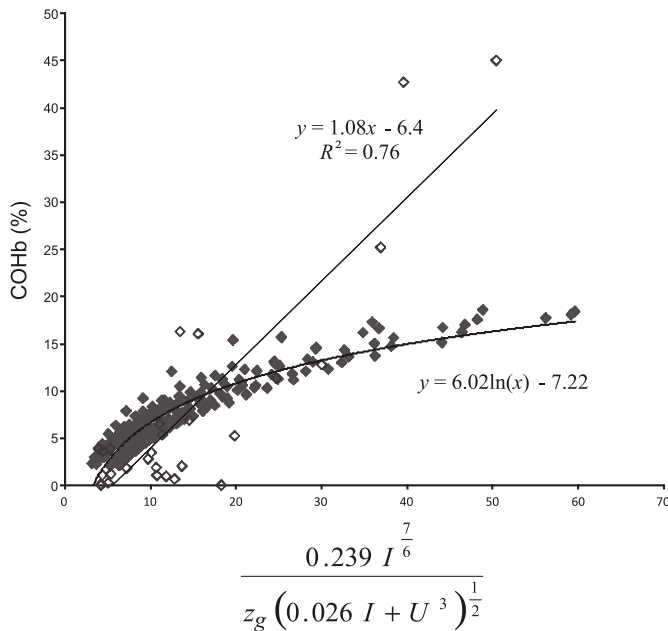
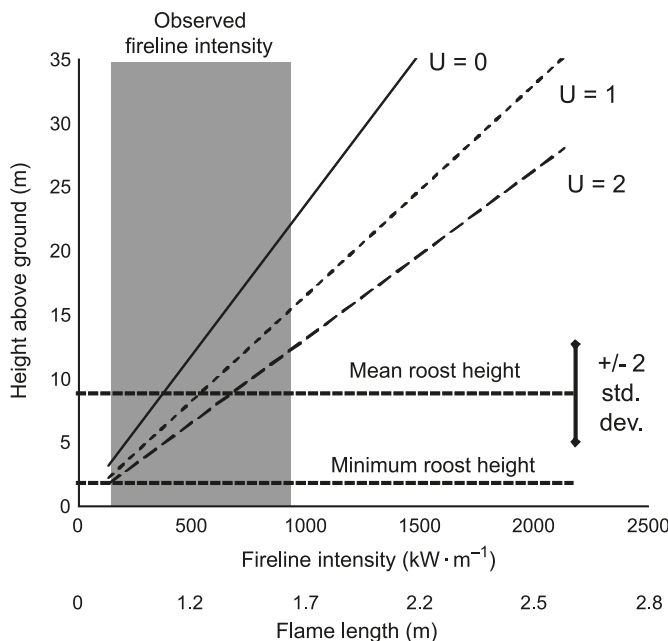


**Fig. 5.** Modeled relationship between the height above ground up to which bat ear burns would be expected and fireline intensity for three ambient wind speeds ( $U$ ) ( $\text{m}\cdot\text{s}^{-1}$ ). The range in fireline intensities estimated across four different prescribed fires is indicated (see Table 3). The minimum (2 m) and mean roosting heights (9.1 m) along with their variability (1 SD = 2.1 m) are shown for male and female Indiana bats (see Dickinson et al. 2009). Approximate flame lengths corresponding to given fireline intensities are provided to facilitate interpretation.



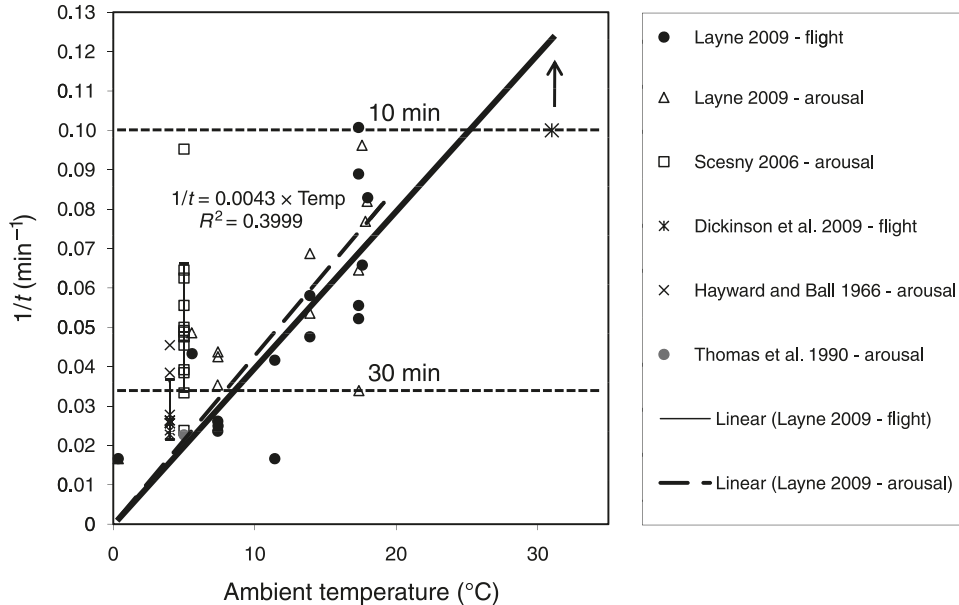
Data from the literature on times to arousal from torpor at a range of ambient temperatures are summarized in Fig. 6. The most relevant data are from Layne’s (2009) study of eastern red bats. He measured time to flight after the bats were exposed to smoke from nearby small-scale leaf litter burns. The only field measurement (Dickinson et al. 2009) indicated that during a warm day (31 °C, Tar Hollow) (Table 3), northern bats flew within 10 min of prescribed fire ignition. The field data from Dickinson et al. (2009) are consistent with an extrapolation of Layne’s trend line to warmer ambient temperatures.

It would be expected that pregnant or lactating female Indiana bats would use torpor less often than males and non-reproductive females because of a need to sustain high metabolic rates. Kurta et al. (1996) demonstrated that adult female Indiana bats in Michigan sustained body temperatures of 35 °C for up to 12 h inside diurnal roosts and that some bats sustained body temperatures at that level for as many as six consecutive days. Maintenance of high body temperatures suggests that these individuals would be able to respond quickly to an oncoming fire. High solar exposure and aggregations of bats at Indiana bat maternity roosts aid in maintaining high body temperatures (USDI Fish and Wildlife Service 2007), yet studies of other bat species have reported declines in body temperatures in reproductively active female bats after diet restriction, such as would happen after poor foraging success in cool or rainy weather (Kurta 1991; Audet and Thomas 1997). Willis et al. (2006) demonstrated multiday bouts of torpor in pregnant female bats during spring storms just prior to giving birth. Thus, at least during cool weather that is otherwise suitable for burning, maternity colonies may be at increased risk from fire because adult females are in torpor. Rainy periods when foraging is poor would not be of concern, since these periods do not provide good burning conditions.

Field studies showed that male and nonreproductive female big brown bats (*Eptesicus fuscus*) select cooler roosts than reproductive females (Hamilton and Barclay 1994) and males enter torpor more regularly than reproductive females (Grinevitch et al. 1995). Given that male Indiana bats tend to roost in smaller trees that are less exposed to solar radiation (Kurta 2005), we assume that male Indiana bats also use torpor regularly. Additional data are needed on roost microclimates and torpor dynamics for bats inside tree roosts as well as their relation to prescribed fire prescriptions to better understand roost site selection (Boyles 2007) and vulnerability of bats to prescribed fire.

Because appropriate plume model validation data are scant in the literature, the accuracy of our integral plume model is uncertain. A comparison of predicted COHb concentrations from field and plume model CO exposures (Fig. 4) indicates that plume model residence times are short compared with residence times of smoke in the field. There are at least two reasons for this result. First, the integral plume model characterizes plumes as arising from a line source of heat generated by flaming combustion. However, a portion of the heat release and smoke emissions from real fires comes from smoldering combustion and residual flaming occurring over long time periods after the passage of the flame front. Second, because our towers were in the interior of prescribed fire units, they were exposed to smoke trans-

**Fig. 6.** Time to arousal and flight as a function of ambient temperature for a range of bat species. Inverse time is plotted to provide a linear relationship. Data are for the little brown bat (*Myotis lucifugus*) (Thomas et al. 1990), big brown bat (*Eptesicus fuscus*) (Hayward and Ball 1966), northern long-eared bat (*Myotis septentrionalis*) (Dickinson et al. 2009), and eastern red bat (*Lasiurus borealis*) (Scesny 2006; Layne 2009). For convenience, the 10 and 30 min arousal times are indicated. The solid line is an extension of the linear fit to Layne's (2009) data on time to flight. The only field measurements are for the northern long-eared bat, which show that two bats with radiotransmitters flew within 10 min of ignition on a warm day (Dickinson et al. (2009)). As a result, 10 min is an underestimate of time to flight as indicated by the arrow. Data from Scesny (2006) and Hayward and Ball (1966) are for 5 °C and are offset for clarity.



ported from beyond the immediate vicinity of the tower. A particularly large contributing area and prolonged exposures to smoke would be expected where heat release in the interior of burn units creates a single, powerful convective column that entrains smoke from a relatively large area (Achtmeier et al. 2004). By contrast, the source area for smoke from the integral plume model is determined by the flame front rate of spread and flame front depth.

Shorter plume model residence times would lead to shorter exposures to CO and thus less COHb accumulation. By contrast, the rapid heat release simulated by the plume model would be expected to result in an overprediction of bat burn injury because the residence times required for injuring thermally thin bat ears (where thickness is 0.16 mm) are short, and rapid heat release results in high plume velocities (and thus higher convection heat transfer coefficients) and higher gas temperatures at a given height.

Because distortion of the plume by ambient wind results in lower temperatures and gas concentrations at height, we expected that wind would ameliorate any heating or gas effects of plumes on bats. Our results with ear burns support this expectation (Fig. 5). Similarly, wind reduced COHb concentrations predicted from plume model data (results not shown). The effects of wind in reducing vegetation heating are well known from both field and model studies (Van Wagner 1973; Mercer and Weber 1994; Kavanagh et al. 2010) and among fire practitioners (e.g., E.J. Bunzendahl, DBNF, personal communication).

Although we did not have gas temperature measurements with which to evaluate the plume model and we find that the model does not conform to reality in important ways,

equating bat ear injury with foliage necrosis (“scorch”) provides both analogy with a commonly observed fire effect and rationale for applying the set of tools developed for predicting foliage necrosis to bat ear injury. Based on plume theory, Van Wagner (1973) first proposed and calibrated a functional relationship between fireline intensity and necrosis height, work that was followed by Gould et al. (1997). Related work on foliage heating in the context of crown fires has also been published (see Cruz et al. 2006a, 2006b). Crown foliage necrosis (whether from foliage, bud, or branch necrosis) is commonly used in predicting the probability of tree mortality from both measured post-fire injury (e.g., McHugh and Kolb 2003) and fire injury predicted from fire behavior and effects models (e.g., Michaletz and Johnson 2008). Foliage necrosis predictions are integral parts of fire effects software designed for use by land managers (Reinhardt 2003; Reinhardt and Crookston 2003).

Uncertainty in our approach to modeling COHb accumulation arises not only from limitations in our field data and uncertainty in our plume model predictions of gas concentrations but also from the lack of information on bat physiology and toxicology. It was not possible for us to use models designed for time-varying CO exposures (e.g., Benignus et al. 1994) because there are no estimates of key physiological parameters and functional relationships for bats. For example, metabolic and breathing rates of bats and other small mammals increase with body temperature during arousal (Hayward and Ball 1966; Fons et al. 1997), although the effects of irritants on those rates can only be surmised. Given a lack of information on irritant effects during torpor, our analysis of COHb accumulation (eq. 9) assumes that

RMV during arousal from torpor is the higher resting value. Because of elevated RMV, our approach may overpredict COHb accumulation. In contrast, dissociation of COHb typically occurs by a two-stage process where the first stage is characterized by more rapid dissociation (Shimazu et al. 2000). We chose to characterize dissociation by a simpler single-stage model that may underestimate dissociation rates and tend to overestimate COHb concentrations. Finally, because of a lack of data in the literature, we extrapolated eq. 9 to [CO] well below 2000 ppm, the lowest [CO] in the data set from which the parameter values in eq. 9 were estimated.

To better understand bat risk in the fire environment, it is clear that additional work is needed on torpor dynamics of roosting bats and the behavior of bats during prescribed fires. Given that our results point to heat effects as the primary concern and gas exposures as secondary, additional research on toxicology of smoke exposures for tree-roosting bats may be of less concern than other issues for the purposes of informing prescribed fire operations on risk mitigation. Our general approach to understanding direct effects of fire on fauna would appear to have applicability across taxa, although the particular characteristics of a species will play a key role (e.g., the models require species-specific parameter values). In an extension of the current paper, work is currently being conducted on smoke exposures of organisms that shelter in tree cavities and subterranean burrows and are thus more sheltered than Indiana bats. This ongoing work may have relevance to faunal survival through fires more intense than those we have considered. Effects of heat and gases on reptiles and birds are largely unexplored.

### Fire management and risk mitigation

Fire managers will be interested in how they can mitigate risk to juvenile and adult tree-roosting bats during prescribed fires because fall and spring burn windows overlap with periods when bats are entering and leaving hibernation. First, ignition operations that proceed slowly at first and, if possible, ensure that smoke is transported over the burn unit before main ignition operations are initiated may provide bats with the sound and smell cues that elicit arousal from torpor. Second, fire managers are well versed in modifying fire behavior by manipulating ignition practices and choosing burning days on which fireline intensities are reduced (Dickinson et al. 2009). An obvious tactic is to avoid a coincidence of upslope wind and upslope spread on dry, south-facing slopes that would produce the most intense burning. Ridge ignition, a tactic used on the DBNF, results in fires that predominantly spread downhill, often against a generalized flow toward ridgelines. Ridge ignition results in a reduction in average fireline intensities relative to other ignition tactics. By contrast, helicopter ignition by distribution of delayed ignition devices combined with hand ignition around burn unit boundaries produces a mix of heading, flanking, backing, and converging firelines exhibiting a wide range of fire behavior and, because of the thorough coverage of ignition, heat and smoke release over a relatively short period of time. Our Tar Hollow prescribed fire was one such burn. Strip head-firing by hand also can lead to areas with intense behavior. In both cases, fireline intensity can be controlled by manipulating the distances between flaming fronts.

Choice of burn season can also reduce fire intensities and thus the risks to bats. Currently, most burning in the mixed-oak forest region within the range of the Indiana bat occurs during the late dormant season and early spring, coinciding with the period when Indiana bats, particularly females, are leaving hibernacula and temperatures are cool. National forests in the central hardwoods region often restrict prescribed burning from mid- to late April (when maternity colonies are forming) through summer (when newborn young may be present in tree roosts) (Dickinson et al. 2009).

Burning during later spring (e.g., late April and early May) has been proposed as a way to accomplish vegetation management objectives at lower fireline intensities than would be needed during winter and early spring, a strategy that could reduce risks for bats. Brose and Van Lear (1998) and Brose et al. (1999) found that single spring burns (late April) were more effective than single winter burns in improving oak advance regeneration in shelterwood stands and in reducing competition for oaks from less fire-tolerant species such as red maple (*Acer rubrum* L.) and yellow-poplar (*Liriodendron tulipifera* L.). Thus, in principle, the proposal has merit, although the authors also found that the benefits of spring fire for oak regeneration increased with fireline intensity. In addition to burn season, stand conditions and fire frequency are critical to success in promoting oak regeneration (Brose et al. 2006). Apart from their effects on oak regeneration, burns later in the spring would generally occur on warmer days during which arousal from torpor would be more rapid (Fig. 6). Effects of late-spring fire disturbance on maternal stress, colony formation, and bat predation risk are largely unknown. A tightening of spring date restrictions will make achieving burn targets more difficult than it is at present, a situation that could be ameliorated by a greater focus on fall burning during the years when that is possible.

In areas with hibernacula, late-winter and early-spring burning has the potential to disturb hibernating bats and cause extra arousals that are energetically costly for bats near the limit of their tolerances (Dickinson et al. 2009). Fire managers in Mammoth Cave National Park attempt to conduct fires on days warm enough to avoid smoke aspiration into hibernacula, i.e., when daytime temperatures are  $>10^{\circ}\text{C}$  (the average cave temperature; USDI National Park Service 2001). Because their prescribed burning season extends from mid-November through April, it may be possible on rare occasions to burn both before bats have emerged from hibernation and when ambient temperatures are  $>10^{\circ}\text{C}$ . In areas with hibernacula, burning in early spring to avoid disturbing maternity colonies must be balanced against risk to hibernating bats.

Roosting behavior of Indiana bats suggests that increasing the numbers of large trees on landscapes that eventually create large (dead) snags for roosting would reduce the risks to bats from fire (Dickinson et al. 2009). Figure 5 shows that bats roosting high in the canopy are at lower risk from exposures to plumes than bats roosting lower on trees. The literature shows that bats roost higher in taller trees and choose larger than average trees from the pool of available snags (Lacki et al. 2009a). Thus, it is reasonable to conclude that allowing more trees to become large on landscapes in which tree-roosting bats live would reduce their risk from fires and, perhaps more importantly, improve maternity habitat.

Mitigating the risks of smoke exposure to bats often can cause conflict with smoke, vegetation, and habitat management. For example, prescribed fire units often are ignited rapidly and in a way that encourages a rapid release of heat and smoke to ensure that smoke is transported up and away from the burn unit as efficiently as possible. Also, relatively high fire intensities may sometimes be desirable to meet vegetation management objectives such as killing trees that compete with fire-tolerant oaks and opening the canopy for oak regeneration (e.g., Iverson et al. 2008). Fires may improve habitat for bats; for instance, a recent study found that nocturnal insect prey abundance increased in the growing season after fire in mixed-oak forest (Lacki et al. 2009b). Understanding the balance between direct negative effects of fire on fauna and long-term positive effects of habitat improvement is a key challenge for research and, added to smoke and vegetation management needs, creates a complicated fire management situation as land managers work to reintroduce fire as a relevant ecological process in eastern US mixed-oak forests (Dickinson et al. 2009).

## Acknowledgements

Thanks to Joe Johnson (Department of Forestry, University of Kentucky) for providing the opportunity to measure bat ear thickness. Helpful comments on the manuscript were provided by E.J. Bunzendahl (US Forest Service, Daniel Boone National Forest) and Becky Ewing (US Forest Service, Region 9). Two anonymous reviewers also provided useful feedback.

## References

- Achtemeier, G.L., Goodrick, S.L., and Liu, Y. 2004. On the multiple-core updraft smoke plume problem: is the genie out of the bottle? 16th Annual International Emission Inventory Conference. Emission Inventories: Integration, Analysis, and Communications, 14–17 May 2007. U.S. Environmental Protection Agency, Raleigh, N.C.
- Andreae, M.O., and Merlet, P. 2001. Emission of trace gases and aerosols from biomass burning. *Global Biogeochem. Cycles*, **15**(4): 955–966. doi:10.1029/2000GB001382.
- Aston, A.R., and Gill, A.M. 1976. Coupled soil moisture, heat and water vapour transfers under simulated fire conditions. *Aust. J. Soil Res.* **14**(1): 55–66. doi:10.1071/SR9760055.
- Audet, D., and Thomas, D.W. 1997. Facultative hypothermia as a thermoregulatory strategy in the phyllostomid bats, *Carollia perspicillata* and *Sturnira lilium*. *J. Comp. Physiol. B Biochem. Syst. Environ. Physiol.* **167**(2): 146–152. doi:10.1007/s003600050058. PMID:9120068.
- Benignus, V.A., Hazucha, M.J., Smith, M.V., and Bromberg, P.A. 1994. Prediction of carboxyhemoglobin formation due to transient exposure to carbon monoxide. *J. Appl. Physiol.* **76**(4): 1739–1745. PMID:8045854.
- Blockley, W.V. 1965. A systematic study human sweat response to activity and environment in the compensable zone of thermal stress. NASA Contract Number 9-3356.
- Bova, A.S., and Dickinson, M.B. 2008. Beyond “fire temperatures”: calibrating thermocouple probes and modeling their response to surface fires in hardwood fuels. *Can. J. For. Res.* **38**(5): 1008–1020. doi:10.1139/X07-204.
- Boyles, J.G. 2007. Describing roosts used by forest bats: the importance of microclimate. *Acta Chiropt.* **9**(1): 297–303. doi:10.3161/1733-5329(2007)9[297:DRUBFB]2.0.CO;2.
- Brose, P.H., and Van Lear, D. 1998. Responses of hardwood advance regeneration to seasonal prescribed fires in oak-dominated shelterwood stands. *Can. J. For. Res.* **28**(3): 331–339. doi:10.1139/cjfr-28-3-331.
- Brose, P.H., Van Lear, D., and Cooper, R. 1999. Using shelterwood harvests and prescribed fire to regenerate oak stands on productive upland sites. *For. Ecol. Manag.* **113**(2–3): 125–141. doi:10.1016/S0378-1127(98)00423-X.
- Brose, P.H., Schuler, T.M., and Ward, J.S. 2006. Responses of oak and other hardwood regeneration to prescribed fire: what we know as of 2005. *In Fire in eastern oak forests: delivering science to land managers*, 15–17 November 2005, Columbus, Ohio. Edited by Matthew B. Dickinson. U.S. For. Serv. Gen. Tech. Rep. NRS-P-1. pp. 123–135.
- Byram, G.M. 1959. Combustion of forest fuels. *In Forest fire: control and use.* Edited by K.P. Davis. McGraw-Hill, New York. pp. 61–89.
- Campbell, G.S., and Norman, J.M. 1998. An introduction to environmental biophysics. Springer, New York.
- Campbell, G.S., Jungbauer, J.D., Jr., Bristow, K.L., and Hungerford, R.D. 1995. Soil temperature and water content beneath a surface fire. *Soil Sci.* **159**(6): 363–374. doi:10.1097/00010694-199506000-00001.
- Cassee, F.R., Arts, J.H.E., Groten, J.P., and Feron, V.J. 1996. Sensory irritation to mixtures of formaldehyde, acrolein, and acetaldehyde in rats. *Arch. Toxicol.* **70**(6): 329–337. doi:10.1007/s002040050282. PMID:8975631.
- Chang, J.C.F., Steinhagen, W.H., and Barrow, C.S. 1981. Effect of single or repeated formaldehyde exposure on minute volume of B6C3F1 mice and F-344 rats. *Toxicol. Appl. Pharmacol.* **61**(3): 451–459. doi:10.1016/0041-008X(81)90368-9.
- Chappell, M.A., and Roverud, R.C. 1990. Temperature effects on metabolism, ventilation, and oxygen extraction in a neotropical bat. *Respir. Physiol.* **81**(3): 401–412. doi:10.1016/0034-5687(90)90120-N. PMID:2259796.
- Clawson, R.L., LaVal, R.K., LaVal, M.L., and Caire, W. 1980. Clustering behavior of hibernating *Myotis sodalis* in Missouri. *J. Mammal.* **61**(2): 245–253. doi:10.2307/1380045.
- Collins, R.F. 1975. A history of the Daniel Boone National Forest 1770–1970. USDA Forest Service, Winchester, Ky.
- Cope, J.B., and Humphrey, S.R. 1977. Spring and autumn swarming behavior in the Indiana bat, *Myotis sodalis*. *J. Mammal.* **58**(1): 93–95. doi:10.2307/1379736.
- Cruz, M.G., Butler, B.W., Alexander, M.E., Forthofer, J.M., and Wakimoto, R.H. 2006a. Predicting the ignition of crown fuels above a spreading surface fire. Part I: model idealization. *Int. J. Wildland Fire*, **15**(1): 47–60. doi:10.1071/WF04061.
- Cruz, M.G., Butler, B.W., and Alexander, M.E. 2006b. Predicting the ignition of crown fuels above a spreading surface fire. Part II: model evaluation. *Int. J. Wildland Fire*, **15**(1): 61–72. doi:10.1071/WF05045.
- Dickinson, M.B., and Johnson, E.A. 2001. Fire effects on trees. *In Forest fires: behavior and ecological effects.* Edited by E.A. Johnson and K. Miyanishi. Academic Press, New York.
- Dickinson, M.B., Lacki, M.J., and Cox, D.R. 2009. Fire and the Indiana bat. *In Proceedings of the 3rd Fire in Eastern Oak Forests Conference*, 20–22 May 2008, Carbondale, Ill.. Edited by Todd Hutchinson. U.S. For. Serv. Gen. Tech. Rep. NRS-P-46. pp. 51–75.
- Diller, K.R., Hayes, L.J., and Blake, G.K. 1991. Analysis of alternate models for simulating thermal burns. *J. Burn Care Rehabil.* **12**(2): 177–189. doi:10.1097/00004630-199103000-00020. PMID:2050731.
- Dupuy, J.L., Marechal, J., and Morvan, D. 2003. Fire from a cy-

- lindrical forest fuel burner: combustion dynamics and flame properties. *Combust. Flame*, **135**(1–2): 65–76. doi:10.1016/S0010-2180(03)00147-0.
- Engstrom, T.R. 2010. First-order fire effects on animals: review and recommendations. *Fire Ecol.* **6**(1): 115–130. doi:10.4996/fireecology.0601115.
- Ernst, A., and Zibrak, J.D. 1998. Carbon monoxide poisoning. *N. Engl. J. Med.* **339**(22): 1603–1608. doi:10.1056/NEJM199811263392206. PMID:9828249.
- Esque, T.C., Schwalbe, C.R., DeFalco, L.A., Duncan, R.B., Hughes, T.J., and Carpenter, G.C. 2003. Effects of desert wildfires on desert tortoise (*Gopherus agassizii*) and other small vertebrates. *Southwest. Nat.* **48**(1): 103–111. doi:10.1894/0038-4909(2003)048<0103:EODWOD>2.0.CO;2.
- Fons, R., Sender, S., Peters, T., and Jürgens, K.D. 1997. Rates of rewarming, heart and respiratory rates and their significance for oxygen transport during arousal from torpor in the smallest mammal, the Etruscan shrew *Suncus etruscus*. *J. Exp. Biol.* **200**(Pt. 10): 1451–1458. PMID:9192497.
- Gates, D.M. 1980. Biophysical ecology. Springer-Verlag, New York.
- Geiser, F. 1986. Thermoregulation and torpor in the Kultarr, *Antechinomys laniger* (Marsupialia: Dasyuridae). *J. Comp. Physiol. B Biochem. Syst. Environ. Physiol.* **156**(5): 751–757. doi:10.1007/BF00692755.
- Gill, M., and Ashton, D.H. 1968. The role of bark type in relative tolerance to fire of three Central Victorian eucalypts. *Aust. J. Bot.* **16**(3): 491–498. doi:10.1071/BT9680491.
- Gooding, G., and Langford, J.R. 2004. Characteristics of tree roosts of Rafinesque's big-eared bat and southeastern bat in northeastern Louisiana. *Southwest. Nat.* **49**(1): 61–67. doi:10.1894/0038-4909(2004)049<0061:COTROR>2.0.CO;2.
- Gould, J.S., Knight, I., and Sullivan, A.L. 1997. Physical modeling of leaf scorch height from prescribed fires in young *Eucalyptus sieberi* regrowth forests in south-eastern Australia. *Int. J. Wildland Fire*, **7**(1): 7–20. doi:10.1071/WF970007.
- Grinevitch, L., Holroyd, S.L., and Barclay, R.M.R. 1995. Sex-differences in the use of daily torpor and foraging time by big brown bats (*Eptesicus fuscus*) during the reproductive season. *J. Zool. (Lond.)*, **235**(2): 301–309. doi:10.1111/j.1469-7998.
- Gross, A.O. 1923. The heath hen. *Auk*, **40**(3): 568–569.
- Guelta, M., and Balbach, H.E. 2005. Modeling fog oil obscurant smoke penetration into simulated tortoise burrows and bat colony trees. ERDC/CERL TR-05-31. U.S. Army Corps of Engineers, Edgewood Chemical Biological Center, Aberdeen Proving Ground, Md.
- Gutsell, S.L., and Johnson, E.A. 1996. How fire scars are formed: Coupling a disturbance process to its ecological effect. *Can. J. For. Res.* **26**(2): 166–174. doi:10.1139/x26-020.
- Hall, J.S. 1962. A life history and taxonomics study of the Indiana bat, *Myotis sodalis*. Sci. Publ. 12. Reading Public Museum and Art Gallery, Reading, Pa.
- Hamilton, J.L., and Barclay, R.M.R. 1994. Patterns of daily torpor and day roost selection by male and female big brown bats (*Eptesicus fuscus*). *Can. J. Zool.* **72**(4): 744–749. doi:10.1139/z94-100.
- Hartzell, G.E., Stacy, H.W., Switzer, W.G., Priest, D.N., and Packham, S.C. 1985. Modeling of toxicological effects of fire gases: IV. Intoxication of rats by carbon monoxide in the presence of an irritant. *J. Fire Sci.* **3**(4): 263–279. doi:10.1177/073490418500300403.
- Hayward, J.S., and Ball, E.G. 1966. Quantitative aspects of brown adipose tissue thermogenesis during arousal from hibernation. *Biol. Bull.* **131**(1): 94–103. doi:10.2307/1539650. PMID:5943781.
- Hobson, C.S., and Holland, J.N. 1995. Post-hibernation movement and foraging habitat of a male Indiana bat, *Myotis sodalis* in western Virginia. *Brimleyana*, **23**: 95–101.
- Holman, J.R. 1986. Heat transfer. McGraw-Hill Book Company, New York.
- Iverson, L.R., Hutchinson, T.F., Prasad, A.M., and Peters, M.P. 2008. Thinning, fire, and oak regeneration across a heterogeneous landscape in the eastern U.S.: 7-year results. *For. Ecol. Manag.* **255**(7): 3035–3050. doi:10.1016/j.foreco.2007.09.088.
- Johnson, E.A. 1992. Fire and vegetation dynamics: studies from the North American boreal forest. Cambridge University Press, Cambridge, U.K.
- Johnson, E.A., and Miyanishi, K. 2001. Forest fires: behavior and ecological effects. Academic Press, New York.
- Jones, J.L., Webb, B.W., Butler, B.W., Dickinson, M.B., Jimenez, D., Reardon, J., and Bova, A.S. 2006. Prediction and measurement of thermally induced cambial tissue necrosis in tree stems. *Int. J. Wildland Fire*, **15**(1): 3–17. doi:10.1071/WF05017.
- Jürgens, K.D., Bartels, H., and Bartels, R. 1981. Blood oxygen transport and organ weights of small bats and small non-flying mammals. *Respir. Physiol.* **45**(3): 243–260. doi:10.1016/0034-5687(81)90009-8. PMID:7330485.
- Kane, L.E., and Alarie, Y. 1977. Sensory irritation to formaldehyde and acrolein during single and repeated exposures in mice. *Am. Ind. Hyg. Assoc. J.* **38**(10): 509–522. doi:10.1080/0002889778507665. PMID:562615.
- Kaplan, H.L., and Hartzell, G.E. 1984. Modeling of toxicological effects of fire gases: I. Incapacitating effects of narcotic fire gases. *J. Fire Sci.* **2**(4): 286–305. doi:10.1177/073490418400200404.
- Kavanagh, K.L., Dickinson, M.B., and Bova, A.S. 2010. A way forward for fire-caused tree mortality prediction: modeling a physiological consequence of fire. *Fire Ecol.* **6**(1): 80–94. doi:10.4996/fireecology.0601080.
- Kim, S.M., Kim, H., and Cho, S.H. 1991. Carboxyhemoglobin dissociation pattern by age in the rat. *Kor. J. Prev. Med.* **24**(4): 507–515.
- Kremens, R.L., Smith, A., and Dickinson, M.B. 2010. Fire metrology: current and future directions in physics-based measurements. *Fire Ecol.* **6**(1): 13–35. doi:10.4996/fireecology.0601013.
- Kurta, A. 1991. Torpor patterns in food deprived *Myotis lucifugus* (Chiroptera: Vespertilionidae) under simulated roost conditions. *Can. J. Zool.* **69**(1): 255–257. doi:10.1139/z91-039.
- Kurta, A. 2005. Roosting ecology and behavior of Indiana bats (*Myotis sodalis*) in summer. In Proceedings of the Indiana Bat and Coal Mining: A Technical Interactive Forum. Edited by K.C. Vories and A. Harrington. Office of Surface Mining, U.S. Department of the Interior, Alton, Ill. Available from www.mcrc.c.osmre.gov/MCR/Resources/bats/pdf/Indiana\_Bat\_and\_Coal\_Mining.pdf [accessed 24 June 2008].
- Kurta, A., Williams, K.J., and Mies, R. 1996. Ecological, behavioural, and thermal observations of a peripheral population of Indiana bats. In Bats and Forests Symposium. Edited by R.M.R. Barclay and R.M. Brigham. B.C. Ministry of Forests, Victoria, B.C.. pp. 102–117.
- Lacki, M.J., Cox, D.R., and Dickinson, M.B. 2009a. Meta-analysis of summer roosting characteristics of two species of *Myotis* bats. *Am. Midl. Nat.* **162**(2): 318–326. doi:10.1674/0003-0031-162.2.318.
- Lacki, M.J., Cox, D.R., Dodd, L.E., and Dickinson, M.B. 2009b. Response of northern bats (*Myotis septentrionalis*) to prescribed fires in eastern Kentucky forests. *J. Mammal.* **90**(5): 1165–1175. doi:10.1644/08-MAMM-A-349.1.
- Lahiri, S. 1975. Blood oxygen affinity and alveolar ventilation in

- relation to body weight in mammals. *Am. J. Physiol.* **229**(2): 529–536. PMID:240284.
- Layne, J.T. 2009. Eastern red bat (*Lasiurus borealis*) response to fire stimulus during torpor. M.S. thesis, Missouri State University, Springfield, Mo.
- Loucks, E., Arthur, M.A., Lyons, J.E., and Loftis, D.L. 2008. Characterization of fuel before and after a single prescribed fire in an Appalachian hardwood forest. *South. J. Appl. For.* **32**(2): 80–88.
- Lunney, D., Gresser, S.M., Mahon, P.S., and Matthews, A. 2004. Post-fire survival and reproduction of rehabilitated and unburnt koalas. *Biol. Conserv.* **120**(4): 567–575. doi:10.1016/j.biocon.2004.03.029.
- McHugh, C.W., and Kolb, T.E. 2003. Ponderosa pine mortality following fire in northern Arizona. *Int. J. Wildland Fire*, **12**: 17–22.
- Mercer, G.N., and Weber, R.O. 1994. Plumes above line fires in a cross wind. *Int. J. Wildland Fire*, **4**(4): 201–207. doi:10.1071/WF9940201.
- Michaletz, S.T., and Johnson, E.A. 2006. Foliage influences forced convection heat transfer in conifer branches and buds. *New Phytol.* **170**(1): 87–98. doi:10.1111/j.1469-8137.2006.01661.x. PMID:16539606.
- Michaletz, S.T., and Johnson, E.A. 2007. How forest fires kill trees: a review of the fundamental biophysical processes. *Scand. J. For. Res.* **22**(6): 500–515. doi:10.1080/02827580701803544.
- Michaletz, S.T., and Johnson, E.A. 2008. A biophysical process model of tree mortality in surface fires. *Can. J. For. Res.* **38**(7): 2013–2029. doi:10.1139/X08-024.
- Moonman, C.E., Russell, K.R., Lohr, S.M., Ellenberger, J.F., and Van Lear, D.H. 1999. Bat roosting in deciduous leaf litter. *Bat Res. News*, **40**(3): 73–75.
- NatureServe. 2009. NatureServe Explorer: an online encyclopedia of life. Version 7.1. Available from [www.natureserve.org/explorer/](http://www.natureserve.org/explorer/) [accessed 11 November 2009].
- Nelson, R.M., Jr. 2002. An effective wind speed for models of fire spread. *Int. J. Wildland Fire*, **11**(2): 153–161. doi:10.1071/WF02031.
- Nielsen, G.D., Bakbo, J.C., and Holst, E. 1984. Sensory irritation and pulmonary irritation by airborne allyl acetate, allyl alcohol, and allyl ether compared to acrolein. *Acta Pharmacol. Toxicol. (Copenh.)*, **54**(4): 292–298. doi:10.1111/j.1600-0773.1984.tb01933.x. PMID:6730984.
- Nowacki, G.J., and Abrams, M.D. 2008. The demise of fire and “mesophication” of forests in the eastern United States. *Bioscience*, **58**(2): 123–138. doi:10.1641/B580207.
- O’Brien, J.J., Stahala, C., Mori, G.P., Callahan, M.A., Jr., and Bergh, C.M. 2006. Effects of prescribed fire on conditions inside a Cuban parrot (*Amazona leucocephala*) surrogate nesting cavity on Great Abaco, Bahamas. *Wilson J. Ornithol.* **118**(4): 508–512. doi:10.1676/05-118.1.
- Purser, D. 1988. Toxicity assessment of combustion products. In *SFPE handbook of fire protection engineering*. 1st ed. Society of Fire Protection Engineers, Boston, Mass. pp. 200–245.
- Reinhardt, E.D. 2003. Using FOFEM 5.0 to estimate tree mortality, fuel consumption, smoke production and soil heating from wildland fire. In *Proceedings of the 2nd International Wildland Fire Ecology and Fire Management Congress and 5th Symposium on Fire and Forest Meteorology*, 16–20 November 2003, Orlando, Fla. American Meteorological Society, Boston, Mass.
- Reinhardt, E.D., and Crookston, N.L. (*Technical Editors*). 2003. The fire and fuels extension to the Forest Vegetation Simulator. U.S. For. Serv. Gen. Tech. Rep. RMRS-GTR-116.
- Rogers, D.F. 1992. *Laminar flow analysis*. Cambridge University Press, Cambridge, U.K.
- Scesny, A.A. 2006. Detection of fire by eastern red bats (*Lasiurus borealis*): arousal from torpor. M.S. thesis, Missouri State University, Springfield, Mo.
- Scesny, A.A., and Robbins, L.W. 2006. Detection of fire by eastern red bats (*Lasiurus borealis*): arousal from torpor. *Bat Res. News*, **47**: 142.
- Schmidt-Neilsen, K., and Larimer, J.L. 1958. Oxygen dissociation curves of mammalian blood in relation to body size. *Am. J. Physiol.* **195**(2): 424–428. PMID:13583188.
- Shimazu, T., Ikeuchi, H., Sugimoto, H., Goodwin, C.W., Mason, A.D., Jr., and Pruitt, B.A., Jr. 2000. Half-life of blood carboxy-hemoglobin after short-term and long-term exposure to carbon monoxide. *J. Trauma*, **49**(1): 126–131. doi:10.1097/00005373-200007000-00019. PMID:10912868.
- Simons, L.H. 1989. Vertebrates killed by desert fire. *Southwest. Nat.* **34**(1): 144–145. doi:10.2307/3671821.
- Speitel, L.C. 1996. Fractional effective dose model for post-crash aircraft survivability. *Toxicology*, **115**(1-3): 167–177. doi:10.1016/S0300-483X(96)03505-6. PMID:9016751.
- Steward, F.R., Peter, S., and Richon, J.B. 1990. A method for predicting the depth of lethal heat penetration into mineral soils exposed to fires of various intensities. *Can. J. For. Res.* **20**(7): 919–926. doi:10.1139/x90-124.
- Szewczak, J.M., and Jackson, D.C. 1992. Ventilatory response to hypoxia and hypercapnia in the torpid bat, *Eptesicus fuscus*. *Respir. Physiol.* **88**(1–2): 217–232. doi:10.1016/0034-5687(92)90042-U. PMID:1626140.
- Thomas, D.W., Dorais, M., and Bergeron, J.M. 1990. Winter energy budgets and cost of arousals for hibernating little brown bats, *Myotis lucifugus*. *J. Mammal.* **71**(3): 475–479. doi:10.2307/1381967.
- USDI Fish and Wildlife Service. 2007. Indiana bat (*Myotis sodalis*) draft recovery plan. First revision. USDI Fish and Wildlife Service, Great Lakes - Big Rivers Region - Region 3, Fort Snelling, Minn.
- USDI National Park Service. 2001. Mammoth Cave National Park Fire Management Plan. Produced by the Office of the Superintendent, Mammoth Cave National Park, Mammoth Cave, Ky.
- Van Wagner, C.E. 1973. Height of crown scorch in forest fires. *Can. J. For. Res.* **3**(3): 373–378. doi:10.1139/x73-055.
- Weise, D.R., and Biging, G.S. 1996. Effects of wind velocity and slope on flame properties. *Can. J. For. Res.* **26**(10): 1849–1858. doi:10.1139/x26-210.
- Wiedinmyer, C., Quayle, B., Geron, C., Belote, A., McKenzie, D., Zhang, X., O’Neill, S., and Wynne, K.K. 2006. Estimating emissions from forest in North America for air quality modeling. *Atmos. Environ.* **40**(19): 3419–3432. doi:10.1016/j.atmosenv.2006.02.010.
- Willis, C.K.R., Brigham, R.M., and Geiser, F. 2006. Deep, prolonged torpor by pregnant, free-ranging bats. *Naturwissenschaften*, **93**(2): 80–83. doi:10.1007/s00114-005-0063-0. PMID:16456644.
- Wooster, M.J., Roberts, G., Perry, G.L.W., and Kaufman, Y.J. 2005. Retrieval of biomass combustion rates and totals from fire radiative power observations: FRP derivation and calibration relationships between biomass consumption and fire radiative energy release. *J. Geophys. Res.* **110**: D24311. doi:10.1029/2005JD006318.